COMMUNICATIONS IN SCIENCE AND TECHNOLOGY
Homepage: cst.kipmi.or.id

On the characterization of EM emission of electronic products: Case study for different program modes

Tito Yuwono[a,*], Mohd Hafiz Baharuddin[b], Hristo Zhivomirov[c], Elyza Gustri Wahyuni[d]

[a]*Department of Electrical Engineering, Islamic University of Indonesia, Yogyakarta 55584, Indonesia*
[b]*Department of Electrical, Electronic and System Engineering, Universiti Kebangsaan Malaysia, Bangi 43600, Malaysia*
[c]*Department of Theory of Electrical Engineering and Measurements, Technical University of Varna, Varna 9010, Bulgaria*
[d]*Department of Informatics, Islamic University of Indonesia, Yogyakarta 55584, Indonesia*

Article history:
Received: 5 October 2023 / Received in revised form: 23 May 2024 / Accepted: 24 May 2024

Abstract

The characterization of the EM emissions for electronic products is crucial to ensure that the emissions have met the requirements of the EMC standards. For this, a more comprehensive testing is required to get more meaningful results. While, the emergence of non-stationary emissions is a challenge to obtain valid analysis results. So far, non-stationary EM emissions is not considered and treated properly in the emission analysis. This paper presents a new method for the analysis of EM emissions from electronic devices as a case study by testing three different program modes (scenarios) of Intel Galileo board. These program modes were designed to vary processing intensity in its memory and processor. A comparison was also made between the actual situation (the presence of non-stationary signals) and the hypothetical situation with the assumption that all emissions were stationary. As a result, a significant difference was observed when the analysis considered the real scenario of a non-stationary emission. The ratio between the average autocorrelation using the proposed algorithm and the average correlation by ignoring the non-stationarity of the emission signal was 113.6 times. The study concludes that different program modes produce the different characteristics of EM emissions, making some of them non-stationary. Hence, we strongly suggest the consideration of the non-stationarity of the EM emissions in characterizing complex electronic devices.

Keywords: Characterization; electronic product; EM emission; program modes; non-stationarity

1. Introduction

The measurement and analysis of electromagnetic (EM) emissions in electronic products is crucial to ensure that the produced emissions have met the EMC requirements and do not interfere with the surroundings. Electronic products that meet EMC standards and regulations can be marketed anywhere, both at national and international level.

Some of the techniques that can be used for the measurement of electromagnetic emissions include Open Area Test Site (OATS) [1–13], Anechoic Chamber (AC) [14–27], Transverse Electromagnetics TEM Cell [28-40], Compact Antenna Test Range (CATR) [41–48], Reverberation Chamber (RC) [49–55] and Near Field Scanning (NFS) [56–74]. A comprehensive review of electromagnetic emission measurements can be found in [75].

Based on [75], NFS has some more advantages compared to other techniques, where it is more economical and is able to locate the source of the emissions. Far field measurements such as OATS, AC, CATR, and RC are not able to detect the sources of the problematic EM emissions. So, it is more difficult to rectify the issue if far field measurement technique is used. One of the main problems in NFS is the presence of non-stationary behavior in the EM emissions. The emergence of this non-stationary emission takes place in a short period with a specific frequency. A previous study dealing with the problem of non-stationary emissions stated that if a non-stationary series were used as an input for predicting the propagation of the EM emissions, the results would be incorrect [76].

Since processes with high emissions may occur only within a small percentage of the time, the averaging process in calculating the field-field correlation will reduce the effect of this process by assuming stationary emission statistics.

The conventional NFS method uses the frequency domain making the emergence of non-stationary emissions unable to be detected, while the new method using the time domain can detect non-stationary EM emission signals. Most of NFS researchers neglect the existence of non-stationary EM emissions. Some examples of NFS studies that ignore non-stationary EM emissions are [77– 80].

Some facts and phenomena of non-stationary emission have been presented in [81]. This non-stationary EM emission is the results of Raspberry Pi 3 and Intel Galileo board measurements [81]. Fig. 1, Fig. 2, and Fig. 3 show the examples of non-stationary EM emissions containing a signal of interest, which

* Corresponding author. Tel.: 0274895287; fax: 0274895007.
Email: tito@uii.ac.id
https://doi.org/10.21924/cst.9.1.2024.1289

causes it to be non-stationary in different ways. In Fig.1 the signal of interest is at the right end and wide, while for EM emissions in Fig. 2 and Fig.3, the signal of interest is narrower. For Fig. 2, the signal of interest is around 0.18ms, and for Fig. 3, the signal of interest around 0.02ms and 1.05ms.

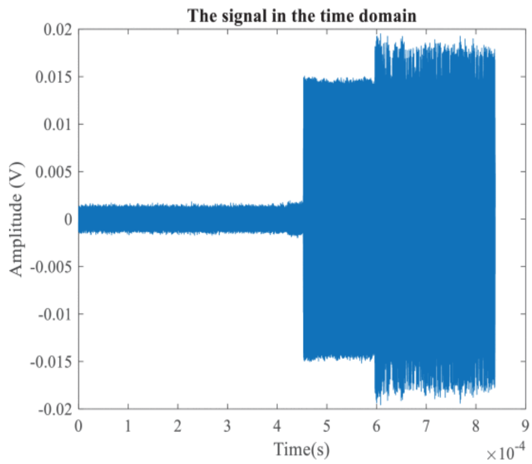

Fig. 1. Non-stationary EM emission from Raspberry Pi 3 [81]

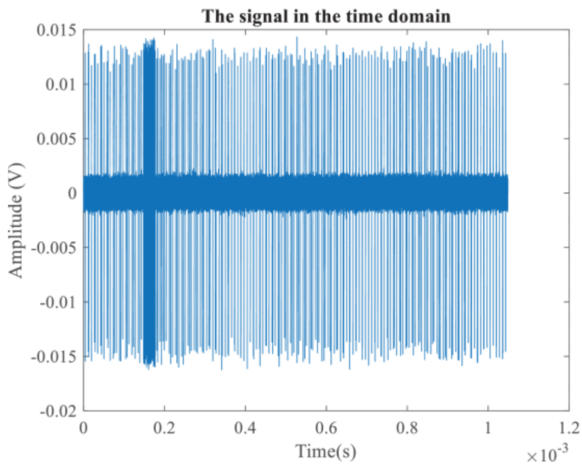

Fig. 2 Non-stationary EM emission from intel Galileo board 1 [81]

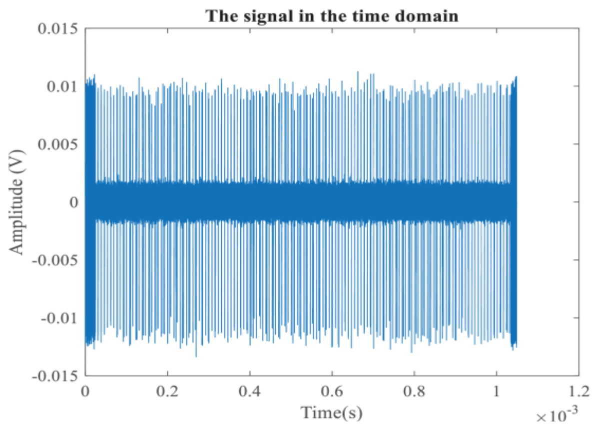

Fig. 3. Non-stationary EM Emission from intel Galileo board 2 [81]

This paper will characterize and analyze the EM emissions from the Galileo board with several program modes that produce stationary and non-stationary EM emissions. The initial hypothesis in this research is that different program modes running in electronic products will produce different emissions. The more complex the program mode being run will produce the different unpredictable EM emission behavior.

The contribution of this research is to improve conventional methods in which in these methods, EM emission analysis is commonly carried out in the frequency domain and does not take into account the non-stationary character of EM emission. In this study, EM emissions analysis was carried out in the time domain and the behavior of EM emissions in certain program modes that were run was studied taking into account non-stationary emissions. The result of the improvement was found more accurate EM emissions and enabled to identify the source of EM emissions in electronic products.

This paper consists of 4 sections. Section 1 presents an introduction related to the phenomenon of non-stationary EM emissions and techniques for measuring EM emissions in electronic products. Section 2 presents the research methodology carried out including the research stages, instruments used as well as research scenarios. Furthermore, Section 3 contains the results and discussion. In this section, the results of EM emission measurements with three different scenarios and analysis of non-stationary EM emissions are discussed. The final section of this paper presents the conclusion of the study results.

2. Materials and Methods

The objective of this study is to characterize EM emissions in electronic products based on different program modes running on the device. To achieve this objective, three research stages were involved: (1) measurement of EM emissions with three program modes (scenarios); (2) stationarity test; and (3) characterization of EM emissions for each scenario.

Fig. 4 shows the process of measuring EM emissions. In this study, the DUT refers to the Intel Galileo board (*cf.* Table 1).

Table 1. Data sheets of Intel Galileo Board [82]

Parameters	Value
Dimensions	123.8 mm (L) x 72.0 mm
Processor	Intel Quark SoC X1000 400 MHz
RAM	256 MB DDR3
Power	7 to 15 Volts
Flash storage	8 KB EEPROM; 8 MB NOR Flash, up to 32-GB microSD card support
Price	$75

The R50-1 RF magnetic probe is manufactured by Langer EMV (*cf.* Table 2).

Table 2. Data sheets of R50-1 Magnetic Probe [83]

Parameters	Value
Head Dimensions	Ø ≈ 10 mm
Frequency range	30 MHz ... 3 GHz
Connector output	SMB, male, jack

Measurements were made by placing the probe tip 2 mm above the Intel Galileo memory. The probe was connected to port 1 of Keysight DSOS804a digital oscilloscope. Table 3 shows the data sheet for this instrument. The sampling rate of this instrument was 20 GSa/s with bandwidth 8 GHz. Based on this data sheet, the instrument can be used to measure EM emissions with the R-50-1 probe, which has a working frequency of 30 MHz - 3 GHz. The setup is shown in Fig. 4.

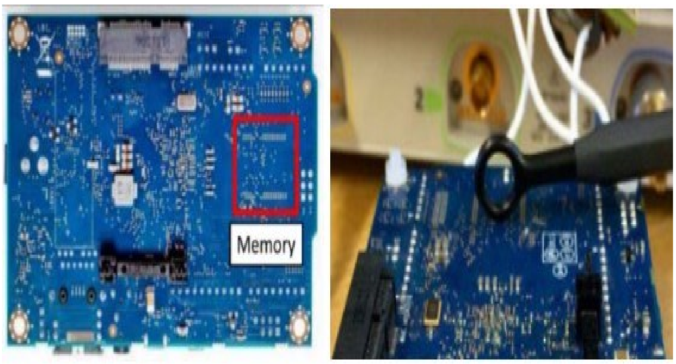

Fig. 4. Measurement process

Table 3. Data sheets of Keysight DSOS804A Digital Oscilloscope [84]

Parameters	Value
Sampling rate	20GSa/s
Number of channels	four
Bandwidth	8 GHz
XGA	15"
ADC	10 bit

The program mode scenario was based on the complexity of the program being run and the use of memory devices and processors:

1. Scenario 1: Galileo performed mathematical calculations.
2. Scenario 2: Galileo processed random numbers stored into a large array of sequential addresses.
3. Scenario 3: Galileo processed random numbers stored into multiple random addresses.

After the measurements, the data were further assessed for stationarity. Since there were only three data sequences only three, the stationarity was estimated by the visual inspection of the run-sequence plots (i.e. the oscillograms). If the EM emission was stationary, then its autocorrelation function was calculated. If the EM emission was non-stationary, a signal of interest that caused it to be non-stationary must be detected. The algorithm to detect the signal of interest was by implementing segmentation and automatic detection based on Short time energy (STE). Based on previous research carried out by the author, STE is the technique with the best performance in segmentation and detection of non-stationary components [81].

In the segmentation process a time-limited windows $w[m]$ extracted the signal frames at regular intervals as [81]

$$x_f[m] = w[m]x[m + fh], \tag{1}$$

where $m \in \{1,...,M\}$ is the local time index, M is the window length, f is the frame index, and h is the hop size.

The STE is defined as the energy of the corresponding signal frame [85]:

$$STE[f] = \sum_m x_f[m]^2 . \tag{2}$$

To analyze the relation of the average signal over the entire signal duration and the maximum amplitude of the signal, we used the autocorrelation function (ACF). The ACF of discrete signal $x[n]$ is expressed as [85] :

$$R_{xx}(l) = \sum_{n=1}^{N-l} x[n]x[n+l], \tag{3}$$

where l is the sample lag introduced between the original signal and its sliding copy.

Fig. 5 shows the flow of this study. The first stage is to measure EM emissions based upon three program modes run by the Intel Galileo board. After obtaining the EM emissions data, the EM emissions were checked to see if they were stationary or non-stationary. If the EM emission was stationary, then it was characterized directly by the autocorrelation operation. If the EM emission was non-stationary, then the STE algorithm was applied for the segmentation process and detection of the part that causes it to be non-stationary. Furthermore, it was characterized using autocorrelation operations.

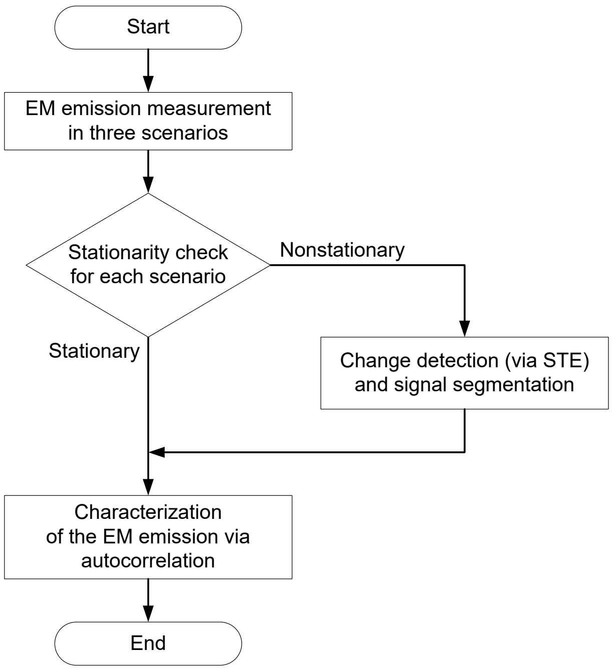

Fig. 5. The EM Emission characterization flow

Three different scenarios were considered while performing the measurement. Each time domain data corresponding to the three scenarios would be checked for stationarity, followed by autocorrelation computation and final characterization. If the signal was estimated as non-stationary, then a change detection parameter was performed, and the signal was segmented into a few stationary portions. In such cases, the autocorrelation was computed for each of them.

3. Results and Discussion

Fig. 6, Fig. 7, and Fig. 8 present the results of measurements in the time domain for Scenario 1, Scenario 2 and Scenario 3, respectively. It is interesting to note that the program mode variation from Intel Galileo produced different EM emissions. Scenario 1 refers to Galileo performing mathematical calculations, which showed that the signal appeared stable without any spikes in EM emissions. Meanwhile, Scenario 2 refers to a process with random numbers filled into a large array of sequential addresses. In this scenario, the EM emission produced had a spike on the edge (red box in Fig. 7). Meanwhile, Scenario 3 showed that Galileo performed one process with random numbers filled into multiple random addresses. Fig. 6 to Fig. 8 show almost the same amplitude. The amplitude of Fig. 6 and Fig. 7 was 0.04 volts, while the amplitude in Fig. 8 was 0.05 Volts. In Fig. 7 there was a visible segment of the emission that had more intensity than other parts (in the red line box making EM emissions non-stationary).

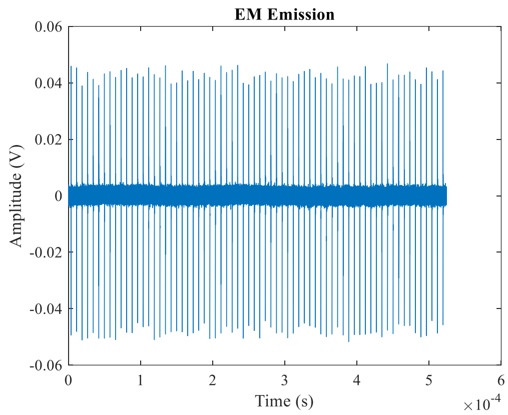

Fig. 6. EM emission in the time domain for scenario 1

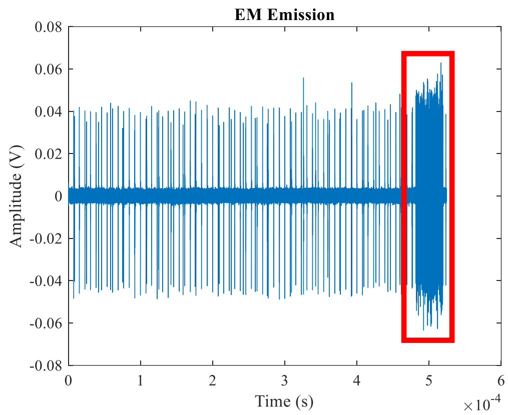

Fig. 7. EM emission in the time domain for scenario 2

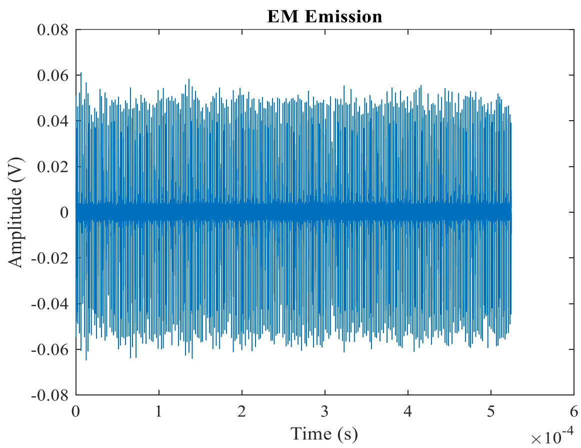

Fig. 8. EM emission in the time domain for scenario 3

The next step was to determine the stationarity of the EM emissions for the three scenarios. The stationarity could visually be estimated (by Eye-ball test) directly in the time domain (*cf.* Figs. 6 to 8). In addition, one may use the spectrograms of the signals of interest for the same goal. The signal is considered stationary if its time or time-frequency domain pattern does not change [86]. The process of stationarity estimation could also be done using the test given in [87].

Fig. 9, Fig. 10 and Fig. 11 show the EM emissions in the time-frequency domain for Scenario 1, Scenario 2 and Scenario 3 respectively. From these three Figures, it was found that the EM emissions of Scenario 1 and Scenario 3 were stationary, while the EM emissions of Scenario 2 were non-stationary.

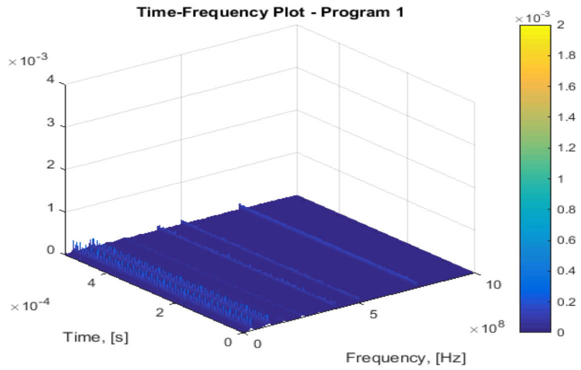

Fig. 9. EM emission in the time-frequency domain for scenario 1

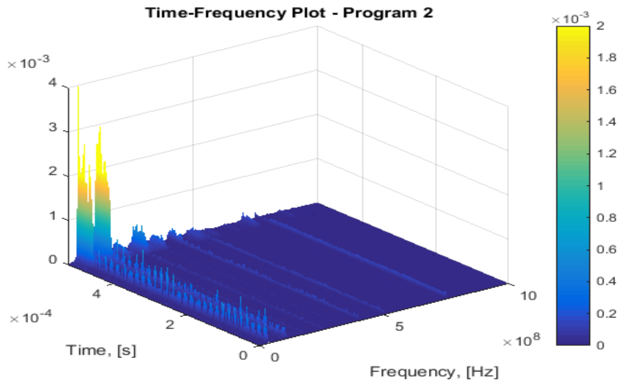

Fig. 10. EM emission in the time-frequency domain for scenario 2

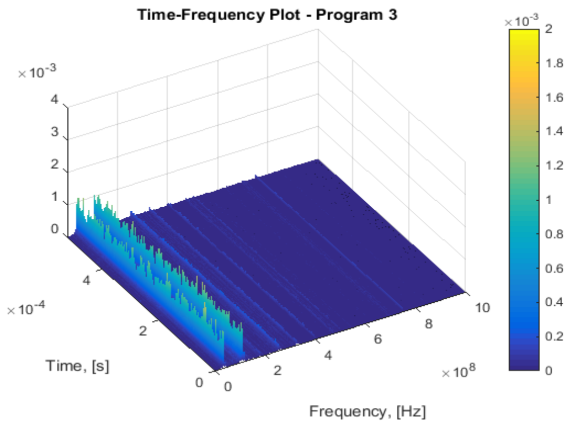

Fig. 11. EM emission in the time-frequency domain for scenario 3

After identifying stationarity, the next step was the autocorrelation operation for stationary emission. This correlation operation was based on equation 3. Fig.12 and Fig.14 show the autocorrelation results for Scenario 1 and Scenario 3. As shown in Fig. 12 and Fig. 14, the ensemble average of the autocorrelation function for Scenario 1 and Scenario 3 was acceptable since the ACF itself was stationary and its average was representative. The maximum peak to average magnitude ratio was found at 1.82 and 2.76 for scenario 1 and scenario 3 respectively.

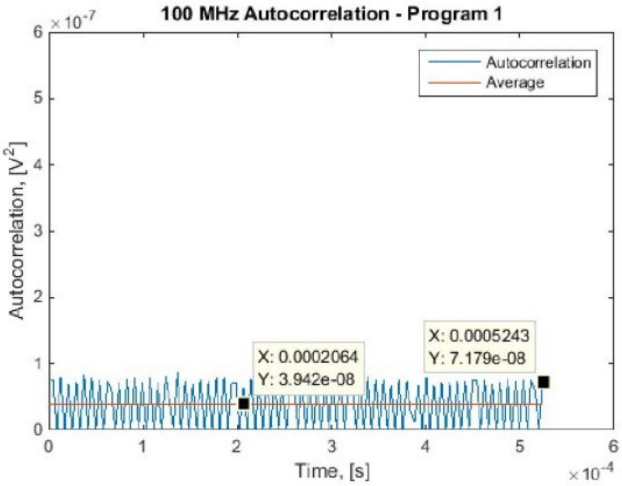

Fig. 12. Autocorrelation and its mean for Scenario 1

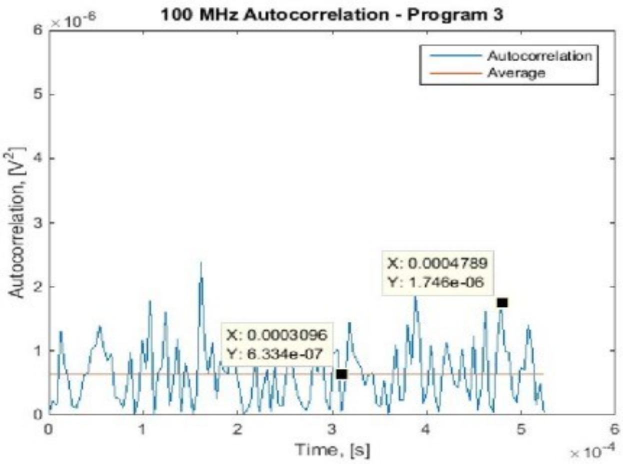

Fig. 13. Autocorrelation and its mean for Scenario 3

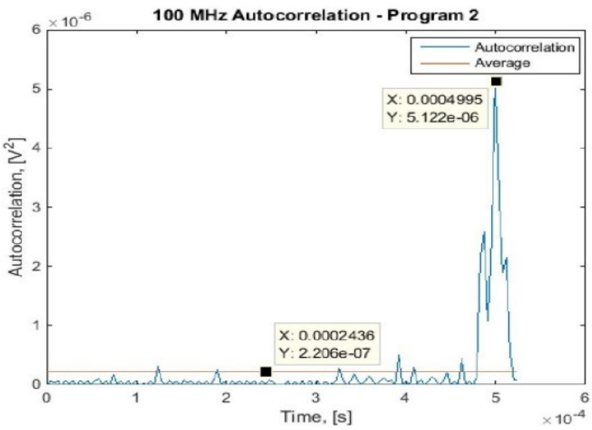

Fig. 14. Auto correlation and its mean for Scenario 2

For EM emissions resulting from Scenario 2, a signal of interest detection operation was required because EM emissions were non-stationary. The results would be biased if we applied autocorrelation directly to EM emission signals from Scenario 2, like Scenario 1 and Scenario 3. In Fig. 14, it can be observed that the average was far below the maximum peak. In other words, there was a high gap between the average value and the maximum peak. The maximum peak to average magnitude ratio was 23.22 for scenario 2. This is in line with previous studies showing that results would be misleading if a non-stationary series was applied as input and considered stationary. The solution is to detect the signal's change points, extract the piecewise stationary segments, and thread them in an ordinary way.

The change detection was performed using the STE property after which the signal was segmented, the results of which are shown in Fig. 15. We can see that the algorithm successfully detected the signals of interest in non-stationary emissions. As shown in Fig. 16, there was a significant difference between the average autocorrelation using the proposed algorithm and the average correlation by ignoring the non-stationarity of the emission signal. In this case, the difference was 113.6 times. Analysis that considers the non-stationary behavior of EM emissions will provide more accurate results. Also, by using autocorrelation, we could determine the source or location of problematic EM emissions precisely. This is very helpful in redesigning electronic products and makes it easier for company to produce electronic products that comply with EMC. The limitations of this method are that it consumes a long-time during measurement, and requires large data and an oscilloscope with a high working frequency (GHz Oscilloscope).

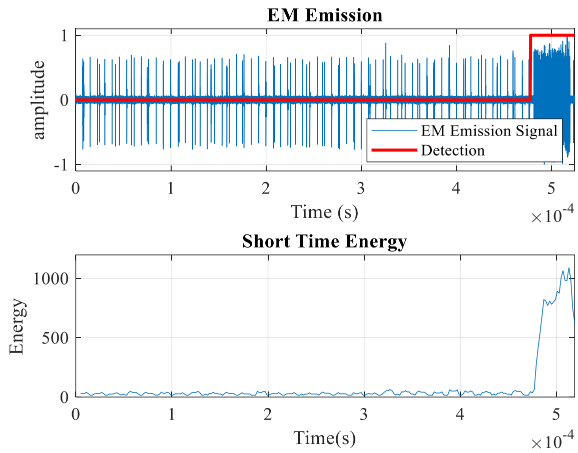

Fig. 15. Detection of the signal of interest using STE

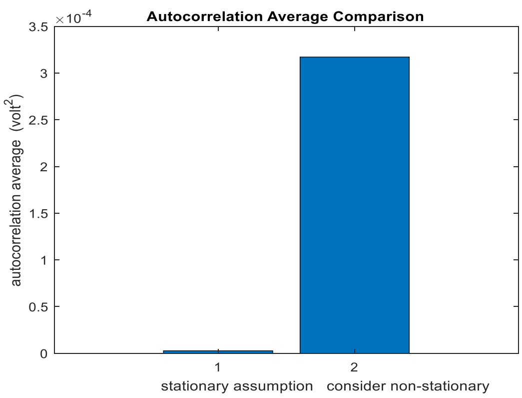

Fig. 16. Autocorrelation mean of EM emission from scenario 2

4. Conclusion

In this paper, EM emissions from an electronic product have been characterized in a new manner in a study organized as a case report. EM emissions produced were found different for each of three program scenarios. The nature of EM emissions was also different; some were stationary, and other were not. It is suggested that to overcome the problem of characterizing the nonstationary EM emissions is by presenting it based upon a change detection via STE feature. Prior to characterization with autocorrelation, nonstationary emissions were segmented, and the signal of interest was detected. The results showed a significant difference between the ACF in the case of stationarity and nonstationarity. Any neglect of this fact leads to a dramatic underestimation of the EM emissions quantitatively and qualitatively. The findings of this research are very useful for obtaining more accurate emission measurements and analysis. This makes it easier for manufacturers to comply with EMC standards. In addition, the manufacturers will be able to determine which components contribute to the problems related to EM emissions, thus making it easier for them to improve the design. This work is a basis for further studies with a larger sample of measurement data. Future research will also more deeply investigate the factors determining the occurrence of nonstationary emissions.

Acknowledgments

The authors would like to acknowledge the financial support from DPPM UII, Directorate General of Higher Education, Research and Technology, Ministry of Education, Culture, Research and Technology, Republic of Indonesia under the Applied Research Grant 2024, Geran Dana Impak Perdana DIP-2021-007), and the Geran Galakan Penyelidik Muda UKM (GGPM-2020-005).

References

1. C. Zombolas, The effects of table material on radiated field strength measurement reproducibility at open area test sites," in IEEE International Symposium on Electromagnetic Compatibility, Montreal, Canada, 2001, pp. 260–264.
2. F. G. Awan and A. Kiran, *Cancellation of Interference for Emission Measurement in Open Area Test Site*, J Measurement, 111 (2017) 183–196.
3. K. M. G. Santos, M. S. Novo, G. Fontgalland, M. B. Perotoni, and C. L. Andrade, *Shielding effectiveness measurements of coaxial cable and connectors using compact open area test site*, J. Microwaves, Optoelectron. Electromagn. Appl., 16 4(2017) 997–1011.
4. S. F. Romero, P. L. Rodriguez, D. E. Bocanegra, D. P. Martinez, and M. A. Cancela, *Comparing Open Area Test Site and Resonant Chamber for Unmanned Aerial Vehicle's High-Intensity Radiated Field Testing*, IEEE Trans. Electromagn. Compat., 60 6(2018) 1704–1711.
5. H. Garbe, How to Reproducibly Measure the Unintended EMEmission from Handheld Devices, 2015 IEEE 5th International Conference on Consumer Electronics Berlin (ICCE-Berlin), Berlin, Germany, 2015, pp. 211–212.
6. Desheng Zhu and Keng Yin Chok, Modeling and correlation of radiated emissions generated in a fully anechoic chamber and at an OATS, IEEE EMC Symposium. International Symposium on Electromagnetic Compatibility, Denver, USA, 1998, pp. 147–152.
7. D. Qiao, Z. Qi, H. Mingliang, and S. Dong-an, Analysis of scattering property of open-area test site ground plane, General Assembly and Scientific Symposium (URSI GASS), Beijing, China, 2014, pp. 1–4.
8. J. R. Regué, M. Ribó, and J. M. Garrell, Radiated emissions conversion from anechoic environment to OATS using a hybrid genetic algorithm - Gradient method, IEEE International Symposium on Electromagnetic Compatibility, Montreal,Canada, 2001, pp. 325–329.
9. J. Park, G. Mun, D. Yu, B. Lee, and W. N. Kim, Proposal of simple Reference Antenna Method for EMI antenna calibration, IEEE International Symposium on Electromagnetic Compatibility, California, USA, 2011, pp. 90–95.
10. D. Meng, Verification of ultra-broadband calculable dipole antennas & applications, 2015 IEEE 12th International Conference on Electronic Measurement and Instruments, ICEMI 2015, Qingdao, China, 2016, pp. 1490–1493.
11. G. Awan, N. M. Sheikh, S. A. Qureshi, and A. Ali, A generic model for the classification of Radiation emission data in electromagnetic compatibility measurement, 2008 IEEE Radio and Wireless Symposium, RWS, Orlando, USA, 2008, pp. 315–318.
12. E. R. Heise and R. E. W. Heise, A method to compute open area test site uncertainty using ANSI C63.4 normalized site attenuation measurement data, Symposium on Electromagnetic Compatibility, Santa Clara, California, 1996, pp. 505–507.
13. Chun Hsiung Chen and Han-Chang Hsieh, A GTD model for open area test site with finite metallic plane, IEEE International Symposium on Electromagnetic Compatibility, Istanbul, Turkey, 2003. EMC '03., 2003, pp. 119-122.
14. S. Tofani, A. Ondrejka, and M. Kanda, *A time-domain method for characterizing the reflection coefficient of absorbing materials from 30 to 1000 MHz*, IEEE Trans. Electromagn. Compat., 33 3(1991) 234–240.
15. B. Fourestié, Z. Altman, and M. Kanda, *Anechoic chamber evaluation using the matrix pencil method*, IEEE Trans. Electromagn. Compat., 41 3(1999)169–174, 1999.
16. Z. Chen and Z. Xiong, Site contributions for radiated emission measurement uncertainties above 1 GHz, 2017 IEEE International Symposium on Electromagnetic Compatibility & Signal/Power Integrity (EMCSI), USA, 2017, pp. 504–509.
17. L.-A. Dina, P.-M. Nicolae, I. D. Smarandescu, and V. Voicu, Considerations on radiated emission measurements for a Laptop in a semi-anechoic chamber, International Conference on Electromechanical and Power Systems (SIELMEN), Lasi, Romania, 2017, pp. 202–207.
18. W. Hofmann, C. Bornkessel, and M. A. Hein, Influence of Electrically Large Structures on the EMC-Compliance of a Semi-Anechoic Chamber, IEEE MTT-S International Conference on Microwaves for Intelligent Mobility (ICMIM), Munich, Germany, 2018, pp. 1–4.
19. Q. Zhang, T. H. Loh, W. Zhang, Y. Yang, Z. Huang, and F. Qin, *A Low-Cost and Efficient Single Probe Based MIMO OTA Measurement Method*, IEEE Trans. Instrum. Meas., 71(2022) 1–15.
20. A. M. Hakimi, A. Keivaan, H. Oraizi, and A. Amini, *Wide-Scanning Circularly Polarized Reflector-Based Modulated Metasurface Antenna Enabled by a Broadband Polarizer*, IEEE Trans. Antennas Propag., 70 1(2021) 84–96.
21. P. Liu, G. F. Pedersen, and S. Zhang, *Wideband Low-Sidelobe Slot Array Antenna With Compact Tapering Feeding Network for E-Band Wireless Communications*, IEEE Trans. Antennas Propag., vol. 70 4(2022) 2676–2685.
22. R. H. Kenney, J. L. Salazar-Cerreno, and J. W. McDaniel, *Two-Dimensional Beam Pattern Synthesis for Phased Arrays With Arbitrary Element Geometry via Magnitude Least Squares Optimization*, IEEE J. Microwaves, 2 2(2022) 337–346,.
23. Z. Tang, F. Yu, W. Rao, S. Lv, Y. Cui, and W. Wang, Electromagnetic Field Tests in the Anechoic Chamber Based on the Shared Tower Scale Model, IEEE 2nd International Conference on Power, Electronics and Computer Applications (ICPECA), Shenyang, China, 2022, pp. 150–153.
24. S. Youn, D. Jang, N. K. Kong, and H. Choo, *Design of a Printed 5G Monopole Antenna With Periodic Patch Director on the Laminated Window Glass*, IEEE Antennas Wirel. Propag. Lett., 21 2(2022) 297–301.
25. Manisha and N. Sood, Validation of anechoic chamber for radiated emission test, 15th Int. Conf. Electromagn. Interf. Compat. INCEMIC 2018, Bangalore, India, pp. 1–4.
26. H. Shida et al., Influence of test table materials on radiated immunity test: Report on investigation using a giant anechoic chamber, in 2018 IEEE Asia-Pacific Symposium on Electromagnetic Compatibility (EMC/APEMC), Singapore, 2018, pp. 572–577.
27. A. M. Silaghi, E. Tolan, A. De Sabata, and A. Buta, Measurement of radiated emissions from an automotive cluster, 12th Int. Symp. Electron. Telecommun. ISETC 2016, Timisoara, Romania, 2016,

pp. 21–24.
28. S. Wen, J. Zhang, and Y. Lv, The optimization design of septum in TEM cells for IC EMC Measurement, 7th Asia-Pacific Conference on Environmental Electromagnetics (CEEM), Hangzhou, China, 2015, pp. 250–253.
29. Y. Li, J. Wu, H. Li, H. Zhang, H. Ma, and J. Wu, Comparison test and error analysis of the TEM cell method in IC radiated emission, IEEE International Symposium on Electromagnetic Compatibility and 2018 IEEE Asia-Pacific Symposium on Electromagnetic Compatibility (EMC/APEMC), Singapore, 2018, pp. 1208–1211.
30. H. M. Pathak, S. Shah, and H. O. Mode, *Development and test analysis of Symmetric Open TEM cell*, J. Sci. Technol. Res., 21 2(2020) 90–97.
31. L. Wen, G. Yalin, and L. Jin, Three new strip-line TEM cells in EMC test, 2016 IEEE International Conference on Electronic Information and Communication Technology (ICEICT), Harbin, China, 2016, pp. 497–500.
32. C. Shi, C. Chai, Y. Yang, Z. Ma, L. Qiao, and X. Yu, *Characterization of electromagnetic field-transmission line coupling of radiated emission and immunity using TEM cell measurement*, Prog. Electromagn. Res. Lett., 64(2016) 65–71.
33. A. V. Demakov and M. E. Komnatnov, Improved TEM-cell for EMC tests of integrated circuits, International Multi-Conference on Engineering, Computer and Information Sciences (SIBIRCON), Novosibirsk, Russia, 2017, pp. 399–402.
34. N. Narang, S. K. Dubey, P. S. Negi, and V. N. Ojha, Precise E-field measurement inside TEM cell at GSM frequencies using microstrip E-field probe, International Conference on Signal Processing and Communication (ICSC), Noida, India, 2016, pp. 126–129.
35. W. Fang et al., *Extracting the Electromagnetic Radiated Emission Source of an Integrated Circuit by Rotating the Test Board in a TEM Cell Measurement*, IEEE Trans. Electromagn. Compat., 61 3 (2019) 833–841.
36. M. Stojanovic, F. Lafon, R. Perdriau, and M. Ramdani, Determination of the coupling model of common mode chokes using a TEM cell, Int. Symp. Electromagn. Compat, Angres, France, 2017, pp. 4–9.
37. H. Jang, J. Lim, Y. Lee, H. Lee, and W. Nah, Electric and magnetic field shielding evaluation of board level shield can using TEM cell, IEEE Electrical Design of Advanced Packaging and Systems Symposium (EDAPS), Seoul, Korea, 2015, pp. 201–204.
38. Y. Bacher et al., A new RLC structure measurement method using a Transverse ElectroMagnetic cell, IEEE International Circuits and Systems Symposium (ICSyS), Langkawi, Malaysia, 2015, pp. 7–10.
39. H. Sinaga and B. H. Sitorus, *Design of tem cell to test the electromagnetic sensor*, ARPN J. Eng. Appl. Sci., 12 12(2017) 3783–3788.
40. C. Shi et al., *Using Termination Effect to Characterize Electric and Magnetic Field Coupling Between TEM Cell and Microstrip Line*, IEEE Trans. Electromagn. Compat., 57 6(2015) 1338–1344.
41. T. M. Gemmer and D. Heberling, *Accurate and Efficient Computation of Antenna Measurements Via Spherical Wave Expansion*, IEEE Trans. Antennas Propag., 68 12(2020) 8266–8269.
42. A. F. Vaquero, M. Arrebola, M. R. Pino, R. Florencio, and J. A. Encinar, *Demonstration of a Reflectarray With Near-Field Amplitude and Phase Constraints as Compact Antenna Test Range Probe for 5G New Radio Devices*, IEEE Trans. Antennas Propag., 69 5(2021) 2715–2726.
43. C. Rowell, B. Derat, and A. Cardalda-Garcia, *Multiple CATR Reflector System for Multiple Angles of Arrival Measurements of 5G Millimeter Wave Devices*, IEEE Access, 8(2020) 211324–211334.
44. S. F. Gregson, C. G. Parini, and S. Pivnenko, Small antenna testing in a compact antenna test range, 41st Annual Symposium of the Antenna Measurement Techniques Association, AMTA, California, USA, 2019, pp. 1–6.
45. Y. Hu, S. Wang, and S. An, Over the air testing and error analysis of 5G active antenna system base station in compact antenna test range, 2019 Photonics Electromagn. Res. Symp. - Fall, PIERS, Xiamen, China, pp. 1007–1010.
46. [J. Zhao and Z. Dong, *Efficient Sampling Schemes for 3-D ISAR Imaging of Rotating Objects in Compact Antenna Test Range*, IEEE Antennas Wirel. Propag. Lett., vol. 15(2016) 650–653.
47. C. Liu and X. Wang, Design ant Test of 0.3 THZ Compact Antenna Test range, Prog. Electromagn. Res. Lett., 70(2017) 81–87.
48. J. Zhao and M. Zhang, Performance 3-D ISAR imaging in compact antenna test range via compressed sensing, in 2017 IEEE 17th International Conference on Communication Technology (ICCT), Chengdu, China, pp. 736–740.
49. A. De Leo, G. Cerri, P. Russo, and V. Mariani Primiani, *A Novel Emission Test Method for Multiple Monopole Source Stirred Reverberation Chambers*, IEEE Trans. Electromagn. Compat., 62, 5(2020) 2334–2337.
50. L. A. Bronckers, K. A. Remley, B. F. Jamroz, A. Roc'H, and A. Bart Smolders, *Uncertainty in Reverberation-Chamber Antenna-Efficiency Measurements in the Presence of a Phantom*, IEEE Trans. Antennas Propag., 68 6(2020) 4904–4915,
51. G. Andrieu, N. Ticaud, F. Lescoat, and L. Trougnou, *Fast and Accurate Assessment of the 'Well Stirred Condition' of a Reverberation Chamber from S11 Measurements*, IEEE Trans. Electromagn. Compat., 61 4(2019) 974–982
52. J. Immidisetti, M. Magdowski, and R. Vick, Retrofitting a Shielded Camera Enclosure with an Internet Protocol Camera and Testing for Radiated Immunity and Emission in a Reverberation Chamber, IEEE Int. Symp. Electromagn. Compat., Singapore, 2018, pp. 849–854.
53. S. Dingjinjin, The Analysis for Multimode of Electrical Fields in Reverberating Chamber, in Intemational Conference on Microwave and Millimeter Wave Technology Proceedings, Beijeng, China, 2004, pp. 923–926.
54. R. Vogt-Ardatjew, U. Lundgren, S. F. Romero, and F. Leferink, *On-Site Radiated Emissions Measurements in Semireverberant Environments*, IEEE Trans. Electromagn. Compat., vol. 59, no. 3, pp. 770–778, 2017, doi: 10.1109/TEMC.2016.2623380.
55. D. Senic et al., *Improved Antenna Efficiency Measurement Uncertainty in a Reverberation Chamber at Millimeter-Wave Frequencies*, IEEE Trans. Antennas Propag., 65 8(2017) 4209–4219.
56. A. Darvish and A. A. Kishk, *Near-Field Shielding Analysis of Single-Sided Flexible Metasurface Stopband TE: Comparative Approach*, IEEE Trans. Antennas Propag., 69 1(2021) 239–253.
57. S. Marathe et al., *Spectrum Analyzer-Based Phase Measurement for Near-Field EMI Scanning*, IEEE Trans. Electromagn. Compat., 62 3(2020) 848–858.
58. S. Lange, D. Schroder, C. Hedayat, C. Hangmann, T. Otto, and U. Hilleringmann, Investigation of the Surface Equivalence Principle on a Metal Surface for a Near-Field to Far-Field Transformation by the NFS3000, International Symposium on Electromagnetic Compatibility - EMC EUROPE, Rome, Italy 2020, pp. 1–6.
59. D. Mandaris et al., Different Test Site Analysis of Radiated Field Measurements of a Complex EUT, International Symposium on Electromagnetic Compatibility - EMC EUROPE, Barcelona, Spain, 2019, pp. 674–679.
60. M. Messer and M. Kühn, Advanced Modeling of an isotropic Three-Axis magnetic field probe using coils and a near field source approach, International Symposium on Electromagnetic Compatibility, Barcelona, Spain, 2019, pp. 173–178.
61. Y. Liu, J. Li, C. Hwang, and V. Khilkevich, *Near-Field Scan of Multiple Noncorrelated Sources Using Blind Source Separation*, IEEE Trans. Electromagn. Compat., 62 4(2020) 1376–1385.
62. H. Ragazzo, D. Prost, F. Issac, S. Faure, J. Carrey, and J. F. Bobo, Thermo-fluorescent images of electric and magnetic near-fields of a High Impedance Surface, Int. Symp. Electromagn. Compat., Barcelona, Spain, pp. 257–260.
63. M. Xiao et al., Spatial resolution measurement of near-field probe by using two adjacent microstrip lines, 12th Int. Work. Electromagn. Compat. Integr. Circuits, Hangzhou, China, 2019, pp. 189–191.
64. G. Langer and J. Hacker, Determining the Emission of a Device from the Near Field of an IC, 12th International Workshop on the Electromagnetic Compatibility of Integrated Circuits (EMC Compo), Hangzhou, China, 2019, pp. 67–69.
65. A.-M. Silaghi, R.-A. Aipu, A. De Sabata, and P.-M. Nicolae, Near-field scan technique for reducing radiated emissions in automotive EMC, IEEE International Symposium on Electromagnetic Compatibility and 2018 IEEE Asia-Pacific Symposium on Electromagnetic Compatibility (EMC/APEMC), Singapore, 2018, pp. 831–836.
66. G. Gradoni et al., *Near-Field Scanning and Propagation of Correlated Low-Frequency Radiated Emissions*, IEEE Trans. Electromagn. Compat., 60 6(2018) 2045–2048.
67. J. Zhou, Y. F. Shu, J. Li, N. Xia, Z. Gu, and X. C. Wei, A measurement verification for EMI source reconstruction method based on amplitude-only near-field scanning, IEEE Int. Symp.

Electromagn. Compat. 2018 IEEE Asia-Pacific Symp. Electromagn. Compat. EMC/APEMC, Singapore, 2018, p. 125, 2018.

68. S. M. Wu et al., Dielectric constant and loss-tangent extraction using near-field technology and phase delay method, 2018 IEEE Int. Symp. Electromagn. Compat. 2018 IEEE Asia-Pacific Symp. Electromagn. Compat. EMC/APEMC, Singapore, 2018, pp. 683–686.
69. H.-N. Lin, C.-H. Wu, J.-F. Huang, W.-D. Tseng, J. Y.-T. Lin, and M.-S. Lin, Near-and far-field shielding effectiveness analysis of magnetic materials and their effect on wireless power charger, 2018 IEEE International Symposium on Electromagnetic Compatibility and 2018 IEEE Asia-Pacific Symposium on Electromagnetic Compatibility (EMC/APEMC), Singapore, 2018, pp. 1071–1076.
70. G. K. Loon and M. H. Baharuddin, *Development of a Magnetic Field Probe for Near-Field Measurement*, 33 4(2021) 853–861.
71. T. Yuwono, M. H. Baharuddin, and T. Yuwono, *High Accuracy Dual Probe Station for Near Field Scanning*, *Bul. Ilm. Sarj. Tek. Elektro*, 5 4(2023)417–426.
72. M. H. Baharuddin *et al.*, Measurement and Wigner function analysis of field-field correlation for complex PCBs in near field, International Symposium on Electromagnetic Compatibility - EMC EUROPE, Wroclaw, Poland, 2016, pp. 7–11.
73. [M. H. Baharuddin *et al.*, Analysis of Nonstationary Emissions for Efficient Characterization of Stochastic EM Fields, International Symposium on Electromagnetic Compatibility (EMC EUROPE), Amsterdam, Netherlands, 2018, pp. 208–213.
74. D. W. P. Thomas, M. H. Baharuddin, C. Smartt, G. Gradoni, G. Tanner, and S. Creagh, Reducing the complexity of near-field scanning of stochastic fields, International Conference on Advanced Technologies, Systems and Services in Telecommunications (TELSIKS), Nis, Serbia, 2017, pp. 11–14.
75. T. Yuwono, M. H. Baharuddin, N. Misran, M. Ismail, and M. F. Mansor, *A review of measurement of electromagnetic emission in electronic product: Techniques and challenges*, Commun. Sci. Technol., 7 1(2022) 23–37.
76. A. Gil, J. Segura, and N. M. Temme, *Numerical Methods for Special Functions*. Society for Industrial and Applied Mathematics, 2007.
77. O. Harwot, Fast near-field characterization of integrated circuits electromagnetic interference, 21st International Conference Radioelektronika 2011, Brno, Czech, 2011, pp. 1–4.
78. F. Xiao, T. Takatsu, K. Murano, and Y. Kami, Complex near electromagnetic field scanning on printed circuit boar*d*, in International Symposium on Electromagnetic Compatibility - EMC EUROPE, Pennsylvania, USA, 2012, pp. 1–4.
79. M. H. Baharuddin, *Measurement and Characterisation of Stochastic Fields*, University of Nottingham, 2019.
80. M. H. Baharuddin, M. T. Islam, T. Yuwono, C. J. Smartt, and D. W. P. Thomas, Impact of Mode of Operations on the Electromagnetic Emissions of a Complex Electronic Device, IEEE International RF and Microwave Conference (RFM), Kuala lumpur, Malaysia, 2020, pp. 1–4.
81. T. Yuwono et al., *Automatic Segmentation of Nonstationary EM Emission of Electronics Product*, IEEE Access, vol. 10 (2022) 40456–40466
82. A. Nayyar and E. V. Puri, *A Review of Intel Galileo Development Board* ' s Technology, Int. J. Eng. Res. Appl., vol. 6 3(2016) 34–39.
83. L. Langer, RF-R 50-1 (H-Field Probe 30 MHz up to 3 GHz), 2022.
84. Keysight, *DSOS404A High-Definition Oscilloscope: 4 GHz, 4 Analog Channels*. https://www.keysight.com/us/en/product/DSOS804A/high-definition-oscilloscope-8-ghz-4-analog-channels.html (accessed Oct. 20, 2023).
85. D. Monolakis and V. Ingle, *Applied Digital Signal Processing*. New York: Cambridge University Press, 2011.
86. B. Boashash, *Time-Frequency Signal Analysis and Processing*. Oxford: Academic Press, 2016.
87. H. Zhivomirov and I. Nedelchev, *A method for signal stationarity estimation*, Rom. J. Acoust. Vib., vol. 17, no. 2, pp. 149–155, 2020.